

Highly Compressible and Superior Low Temperature Tolerant Supercapacitors based on Dual Chemically Crosslinked PVA Hydrogel Electrolytes

Zhenzhen Liu, Junmei Zhang, Jing Liu, Yanjun Long, Liming Fang, Qingwen Wang,*
Tao Liu*

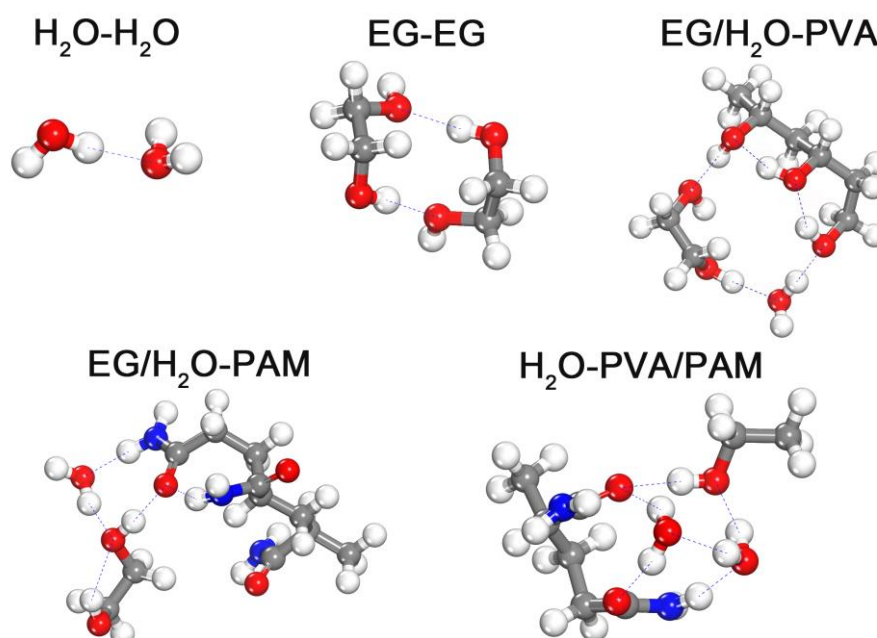


Figure S1. DFT modeling of H₂O-H₂O, EG-EG, EG/H₂O-PVA, EG/H₂O-PAM and H₂O-PVA/PAM.

Table S1. DFT calculation results of the interaction energy of different system.

Model	Interaction energy (eV)	Interaction energy (Kcal/mol)
H ₂ O-H ₂ O	-0.25	-5.78
EG-H ₂ O	-0.45	-10.40
EG-EG	-0.83	-8.71
PVA-PAM	-0.52	-12.03
EG/H ₂ O-PVA	-1.47	-33.93
EG/H ₂ O-PAM	-1.30	-30.04
H ₂ O-PVA/PAM	-1.61	-37.03
EG/H ₂ O-PVA/PAM	-1.90	-43.94
EG/H ₂ O-PVA/PAM	-1.78	-41.16

Table S2. The compressive mechanical properties of SN/DN hydrogels.

Sample Code	Fracture Stress/MPa	Fracture Stain/%	E/MPa
SN	0.14	73.3	0.0211
DN 1.5+EG	0.60	77	0.0461
DN 2+EG	1.50	80.2	0.0375
DN 2.5+EG	3.50	79.8	0.0523
DN 3+EG	2.40	79.6	0.0869
DN 2.5-EG	0.66	65.5	0.0698

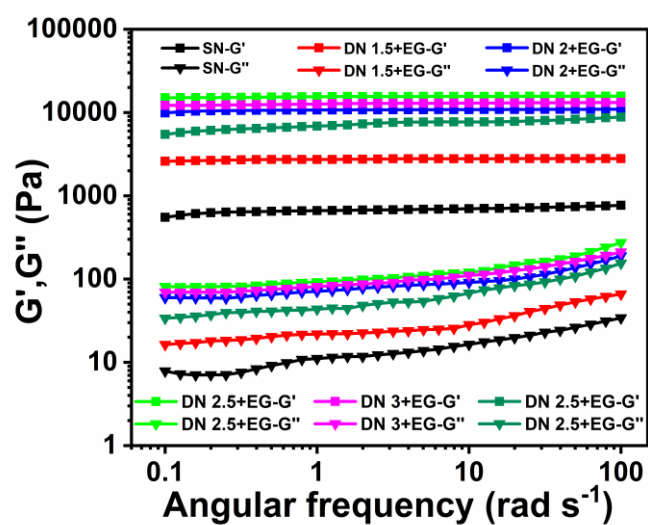


Figure S2. The storage modulus (G') and loss modulus (G'') of SN, DN+EG, DN-EG hydrogels.

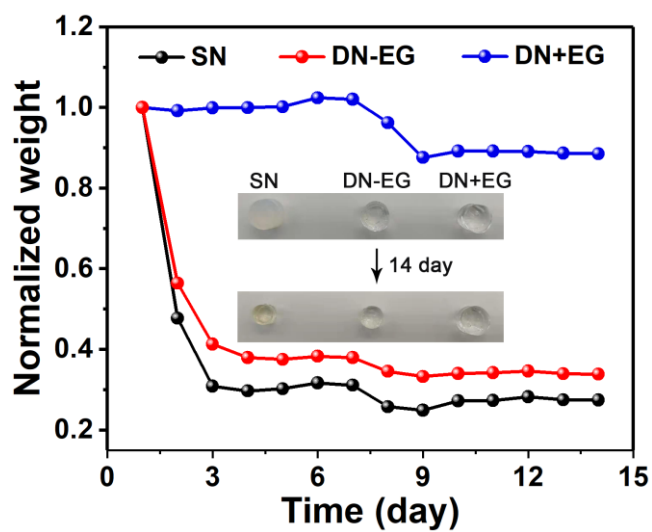


Figure S3. Normalized weight retention of the SN, DN 2.5-EG, DN 2.5+EG hydrogels kept at RT in atmosphere environment.

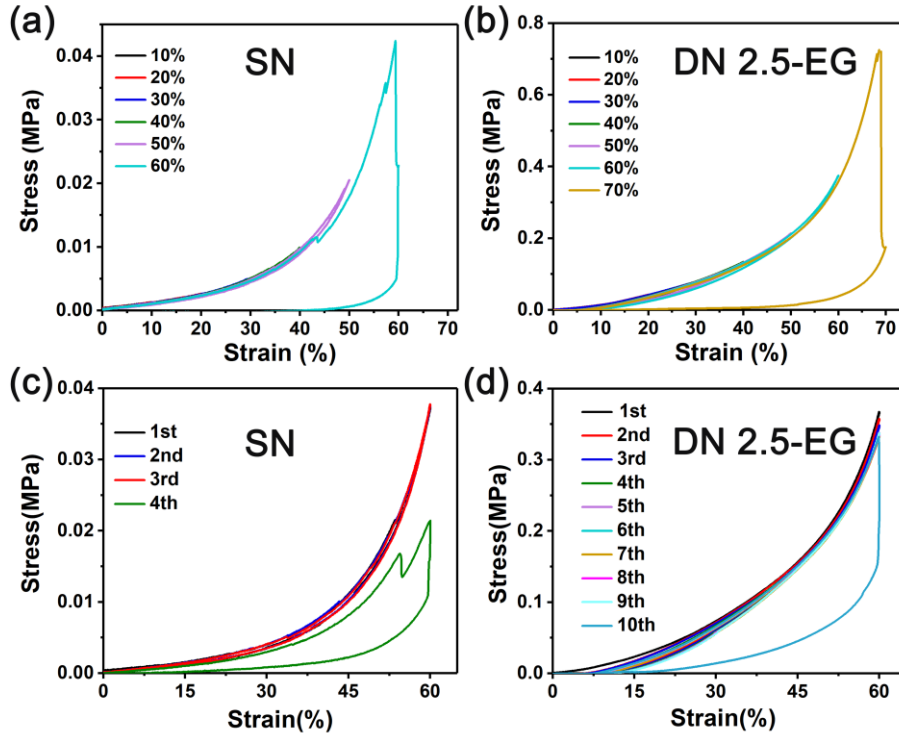


Figure S4. Successive stress-strain curves by varying the maximum compression strain for SN (a) and DN 2.5-EG hydrogels (b). Cyclic compressive stress-strain curves at 60% strain under loading-unloading mechanical test for SN (c) and DN 2.5-EG hydrogels (d).

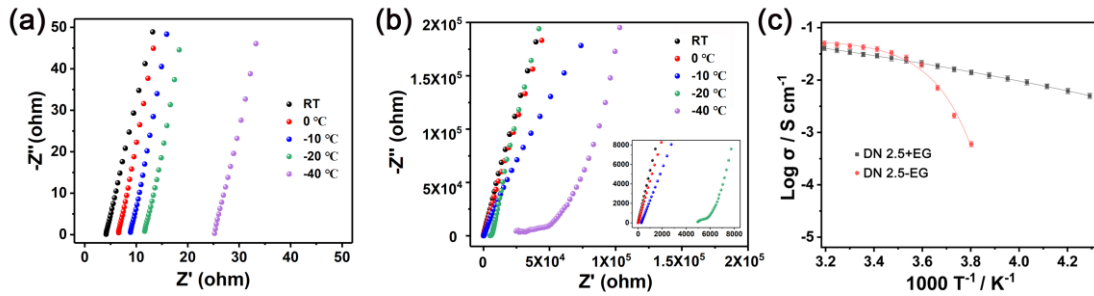


Figure S5. The Nyquist plot of DN 2.5+EG (a) and DN 2.5-EG (b) hydrogel electrolyte under different temperatures. (c) Temperature dependence of ionic conductivity of the above two different hydrogel electrolytes.

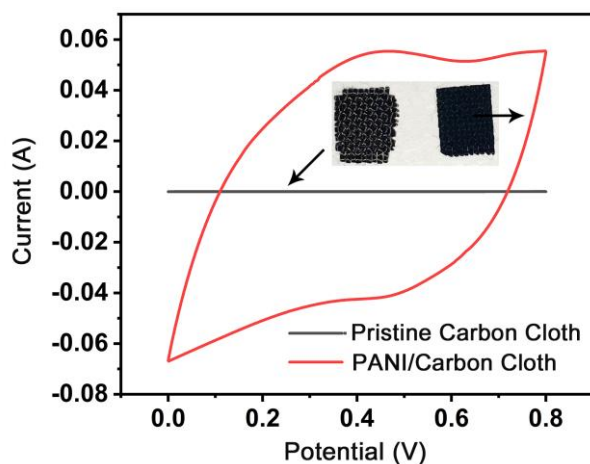


Figure S6. The CV curves of PANI deposited carbon cloth electrode (PANI/Carbon Cloth) and pristine carbon cloth.

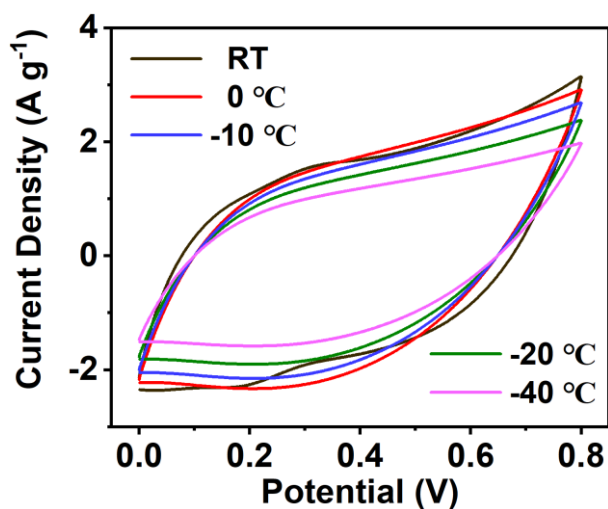


Figure S7. The CV curves of DN 2.5+EG hydrogel based supercapacitors under different temperatures.

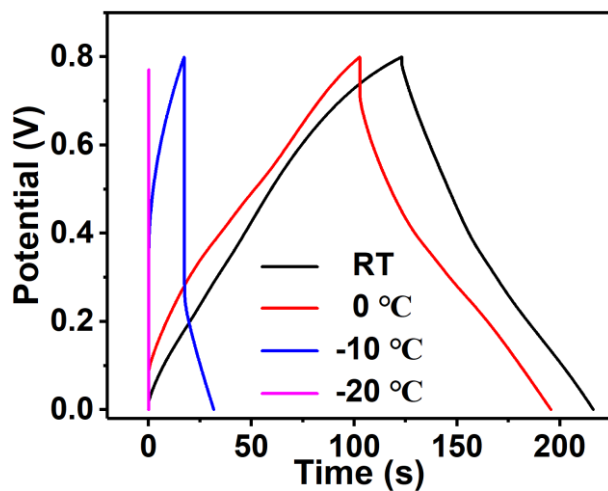


Figure S8. The GCD curves of DN 2.5-EG hydrogel based supercapacitors under different temperatures

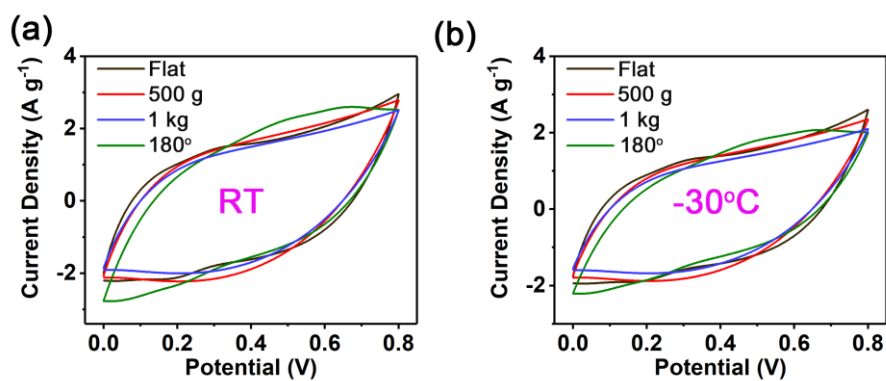


Figure S9. The CV curves of DN 2.5+EG hydrogel based supercapacitors under different load-bearing condition at RT (a) and -30 °C (b).

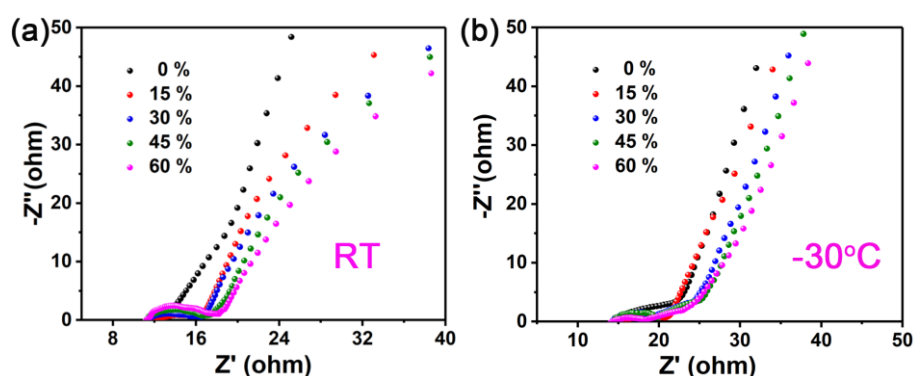


Figure S10. The Nyquist plots of supercapacitors based on DN 2.5+EG hydrogel electrolyte under different compressive strain at RT (a) and -30°C (b).

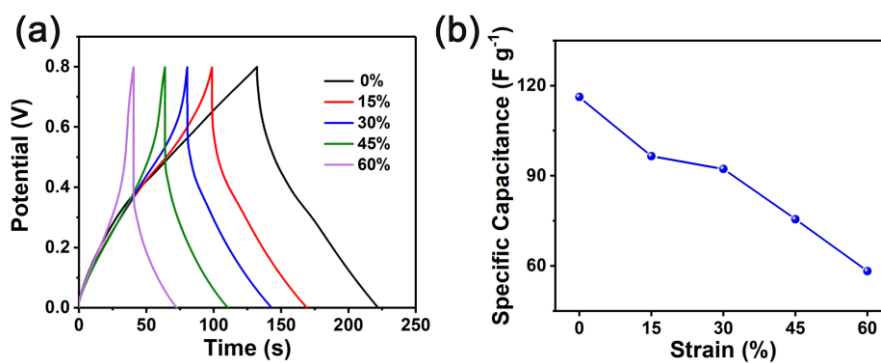


Figure S11. GCD curves of supercapacitors based on DN 2.5-EG hydrogel electrolytes under different compressive strain (a), and the corresponding specific capacitance (b).

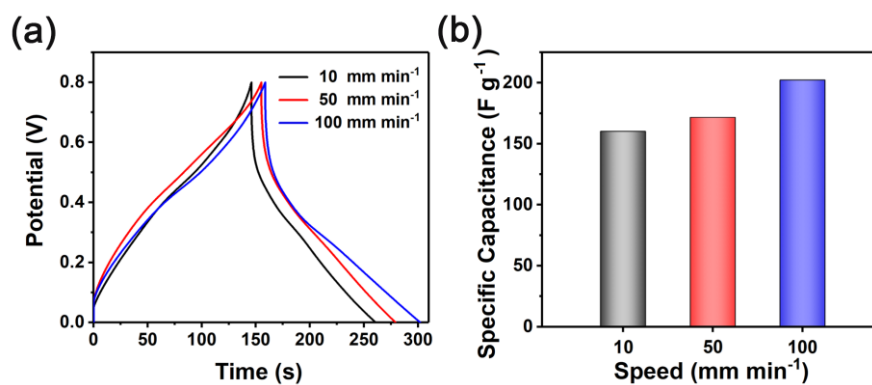


Figure S12. GCD curves of supercapacitors based on DN 2.5+EG hydrogel electrolytes after different high compressing speed (a), and the corresponding specific capacitance (b).

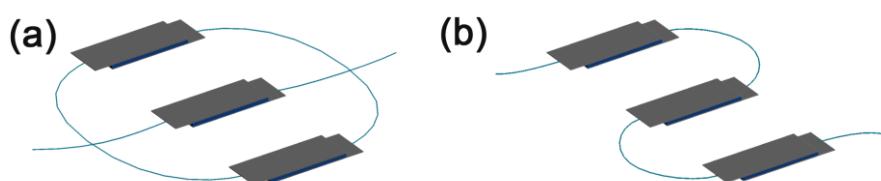


Figure S13. Schematic illustration of supercapacitors in parallel (a) and in series (b).



Figure S14. (a) Photographs of electrical clock powered by two devices in series in compressing state. Photographs of LED lamp powered by three devices in series in compressing state (b) and bending state (c).

Table S3. Comparison of different SCs in Recent Reports

Reference	Electrolyte	Electrode	Cell Specific Capacitance (<i>RT</i> , F g ⁻¹)	Temperature (°C)	Cell Specific Capacitance (<i>LT</i> , F g ⁻¹)	Ionic Conductivity (S cm ⁻¹)
this work	PVA-PAM-ethylene glycol	PANI/carbon cloth	185.1 (0.5 A g ⁻¹)	-40	150.1 (0.5 A g ⁻¹)	0.48
[1]	PVA- <i>g</i> -TMAC	activated carbon	89 (1 A g ⁻¹)	N/A	N/A	0.0642
[2]	Li-AG-PAM	activated carbon	21.175 (0.2 A g ⁻¹)	N/A	N/A	0.041
[3]	PVA-boronic	PANI/ carbon cloth	153 (0.25 A g ⁻¹)	N/A	N/A	0.1
[4]	CMC/Li ₂ SO ₄	activated carbon	73.95 (0.2 A g ⁻¹)	N/A	N/A	0.0535
[5]	cellulose/Li ₂ SO ₄	Lig/SWCNT _{HNO₃}	73 (0.5 A g ⁻¹)	N/A	N/A	N/A
[6]	Lignin/KOH	lignin/PAN carbon nanofiber	129.23 (0.5 A g ⁻¹)	N/A	N/A	0.01035
[7]	SA- <i>g</i> -DA/KCl	activated carbon	97 (1 A g ⁻¹)	-10	79.5 (1 A g ⁻¹)	0.1197
[8]	MGO-PAM	M-PANI film	89.05 (0.1 A g ⁻¹)	-30	70.85 (0.5 A g ⁻¹)	0.127
[9]	PVA-KC	activated carbon	117.5 (0.5 A g ⁻¹)	-40	89 (0.2 A g ⁻¹)	0.21

References

1. Z. Wang and Q. Pan, *Adv. Funct. Mater.*, 2017, **27**, 1700690.
2. T. Lin, M. Shi, F. Huang, J. Peng, Q. Bai, J. Li and M. Zhai, *ACS Appl. Mater. Interfaces*, 2018, **10**, 29684-29693.
3. W. Li, F. Gao, X. Wang, N. Zhang and M. Ma, *Angew. Chem., Int. Ed.*, 2016, **128**, 9342-9347.
4. J. Wei, J. Zhou, S. Su, J. Jiang, J. Feng, Q. Wang, *ChemSusChem*, 2018, **11**, 3410-3415.
5. Z. Peng, Y. Zou, S. Xu, W. Zhong, W. Yang, *ACS Appl. Mater. Interfaces*, 2018, **10**, 22190-22200.
6. J. H. Park, H. H. Rana, J. Y. Lee, H. S. Park, *J. Mater. Chem. A*, 2019, **7**, 16962-16968.
7. F. Tao, L. Qin, Z. Wang and Q. Pan, *ACS Appl. Mater. Interfaces*, 2017, **9**, 15541-15548.
8. X. Jin, G. Sun, G. Zhang, H. Yang, Y. Xiao, J. Gao, Z. Zhang and L. Qu, *Nano Research*, 2019, DOI: 10.1007/s12274-019-2382-z.
9. X. Hu, L. Fan, G. Qin, Z. Shen, J. Chen, M. Wang, J. Yang and Q. Chen, *J Power Sources*, 2019, **414**, 201-209.